Modeling and Simulation of a STATCOM for reactive power control

Anshu Prakash Murdan
Department of Electrical and Electronic Engineering
University of Mauritius
Reduit, Mauritius
a.murdan@uom.ac.mu

Iqbal Jahmeerbacus
Department of Electrical and Electronic Engineering
University of Mauritius
Reduit, Mauritius
iqbal@uom.ac.mu

S Z Sayed Hassen
Department of Electrical and Electronic Engineering
University of Mauritius
Reduit, Mauritius
z.sayedhassen@uom.ac.mu

2022 4th International Conference on Emerging Trends in Electrical, Electronic and Communications Engineering (ELECOM) | 978-1-6654-6697-4/22/$31.00 ©2022 IEEE | DOI: 10.1109/ELECOM54934.2022.9965258

***Abstract*—Reliable and efficient power systems operation requires voltage control as well as minimal reactive power flow between a load and the grid. To achieve this objective, reactive power compensating devices are typically utilized. In modern power systems, the synchronous static compensator (STATCOM) is primarily used for reactive power control, both in distribution and transmission lines. This study presents the modeling and simulation of a STATCOM based on a voltage source converter. Simulations are performed for both single phase and three phase power systems. Furthermore, two control techniques, utilizing Proportional Integral (PI) as well as Proportional Resonant (PR) controllers are explored. The PR controller presents several advantages compared to the PI controller. Simulation results show that in both cases, the STATCOM, connected in shunt with the load either provides reactive power to the load, or absorbs reactive power from the load. Thus, net reactive power transfer from the grid to the load is zero. The grid provides only active power, thus keeping the power factor to almost unity.**

Keywords— STATCOM, Proportional Integral, Proportional Resonant, voltage source inverter

I. INTRODUCTION

A fault on a long distribution feeder may cause significant voltage fluctuations at the load bus. Reactive power compensating devices are typically used to improve the voltage profile. These compensating devices include shunt capacitors, static VAR compensators (SVC)[1], as well as static synchronous compensators (STATCOM)[2]. However, STATCOMs have proved to be more efficient for voltage regulation [3], [4]. STATCOMs have also found wide applications in power systems for enhancing power quality, damping oscillations, and increasing the stability margin[1]. Today's power systems are highly characterized with increasing penetrations of variable renewable energy sources like solar PV and wind systems. This growth puts additional pressures on voltage control and reactive power compensation. Several countries have implemented grid codes that require wind farms to participate in voltage support, in order to improve power quality. In this paper, we investigate the use of a STATCOM for reactive power transfer for a single phase as well as a three-phase power system, for voltage regulation. Many researchers have explored the use of STATCOMs in wind farms. In [5], a solution was proposed for constant speed turbine wind farms, whereby a STATCOM was used along with series impedances and a braking resistor, for grid voltage support. The compliance with grid codes was studied under harsh disturbances. More recently, authors of [6] investigated the impact of integrating a doubly-fed induction generator (DFIG) based wind park with a STATCOM, on the high voltage ride-through capability. STATCOMs have also found applications in grid connected photovoltaic (PV) systems. In [7], a grid connected PV source was integrated with a distribution STATCOM, and a control scheme was devised that provided maximum power point tracking capability, and unity power factor.

II. METHODOLOGY

A. Working principle of a STATCOM

The STATCOM can be implemented using either a voltage source converter (VSC) or a current source converter (CSV), in order to modulate its reactive power output [8], [9]. In this paper we consider a VSC-based STATCOM. The working principle of a STATCOM is illustrated in Fig. 1.

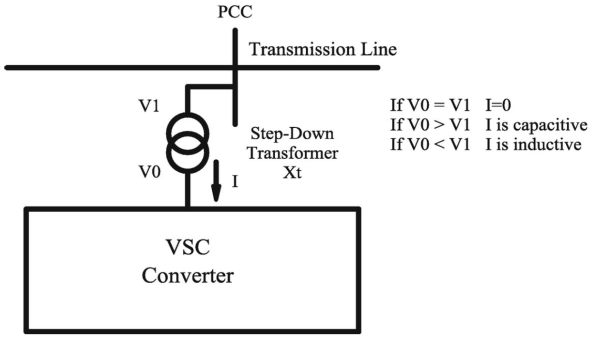

Fig. 1. Schematic diagram of a STATCOM

The reactive power Q can be expressed as:

$$Q = \sqrt{3}.V_1.I = \sqrt{3}.V_1.\frac{(V_0 - V_1)}{X_t} \quad (1)$$

where V_0 : output voltage from the VSC,

V_1 : Grid voltage at the point-of-common-coupling (PCC),

I : Current into transformer on the VSC side, and

X_t: Equivalent reactance of the transformer.

B. Voltage Source Converter Model

A VSC can typically be implemented through the use of a constant dc voltage source, that is either a battery or a capacitor. The direction of the current flow dictates whether power is supplied or absorbed into the converter. Fig. 2 shows the schematic of a three-phase VSC.

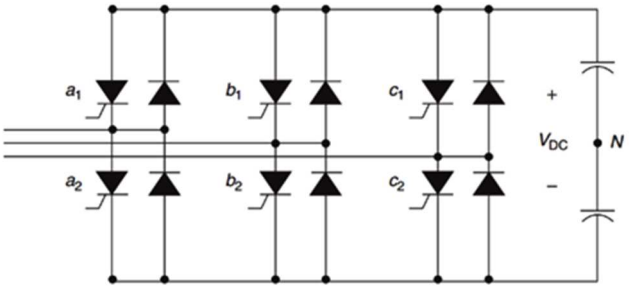

Fig. 2. Three-phase, full-wave voltage source converter

C. Switching Pattern

The typical switching pattern of the VSC is such that $a_1 = \overline{a_2} = a$, $b_1 = \overline{b_2} = b$ and $c_1 = \overline{c_2} = c$. The switching patterns influence the resulting voltage waveforms. For example, if $a\ b\ c = 1\ 1\ 0$, the resulting topology of the converter can be depicted as shown in Fig. 3. Herein $V_{ab} = 0$, $V_{bc} = V_{DC}$ and $V_{ca} = -V_{DC}$ (highlighted). All possible switching combinations are given in TABLE I. In this paper, the 'sine-triangle' method is used for generating the pulse width modulated (PWM) signals.

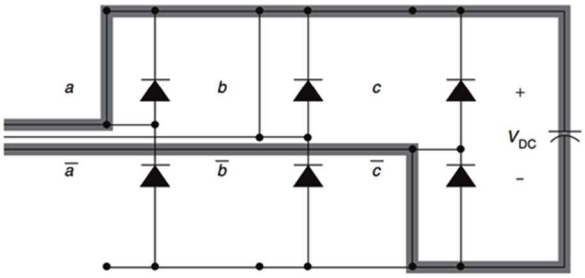

Fig. 3. Three-phase, full-wave VSC, with Switch a ON, Switch b ON, and Switch c OFF

TABLE I. VSC SWITCHING STATES

Switch			Voltage		
a	*b*	*c*	V_{ab}	V_{bc}	V_{ca}
0	0	0	-	-	-
0	0	1	0	$-V_{DC}$	V_{DC}
0	1	0	$-V_{DC}$	V_{DC}	0
0	1	1	$-V_{DC}$	0	V_{DC}
1	0	0	V_{DC}	0	$-V_{DC}$
1	0	1	V_{DC}	$-V_{DC}$	0
1	1	0	0	V_{DC}	$-V_{DC}$
1	1	1	-	-	-

D. STATCOM equivalent circuit

Reactive power is supplied to the grid from the STATCOM when a current is injected in quadrature with the grid voltage. Fig. 4 shows the equivalent model of a voltage source converter connected to the three-phase AC system through a series impedance [5].

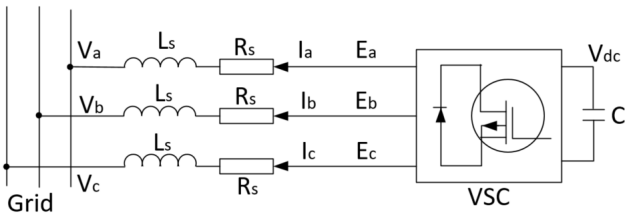

Fig. 4. Equivalent circuit of the STATCOM

In most converters, the series impedance is often equivalent to the leakage reactance of a power transformer. In the abc reference frame, the AC-side circuit equations can be written by applying KVL:

$$L_s \frac{d}{dt}\begin{bmatrix} I_a \\ I_b \\ I_c \end{bmatrix} = \begin{bmatrix} -R_s & 0 & 0 \\ 0 & -R_s & 0 \\ 0 & 0 & -R_s \end{bmatrix}\begin{bmatrix} I_a \\ I_b \\ I_c \end{bmatrix} + \begin{bmatrix} E_a - V_a \\ E_b - V_b \\ E_c - V_b \end{bmatrix} \quad (2)$$

Transforming equation (2) into the synchronous $dq0$ frame of reference gives:

$$\frac{d}{dt}\begin{bmatrix} I_d \\ I_q \\ I_0 \end{bmatrix} = \begin{bmatrix} \frac{-R_s}{L_s} & \omega_e & 0 \\ -\omega_e & \frac{-R_s}{L_s} & 0 \\ 0 & 0 & \frac{-R_s}{L_s} \end{bmatrix}\begin{bmatrix} I_d \\ I_q \\ I_0 \end{bmatrix} + \frac{1}{L_s}\begin{bmatrix} E_a - V_a \\ E_b - V_b \\ E_c - V_b \end{bmatrix} \quad (3)$$

The real and reactive power equations under the rotating $dq0$ reference frame are given as shown in equations (4) and (5).

$$P = \frac{3}{2}(V_d I_d + V_q I_q) \quad (4)$$

$$Q = \frac{3}{2}(V_d I_q - V_q I_d) \quad (5)$$

E. Control of STATCOM

STATCOMs can be controlled using two contrasting control schemes [10], namely the Type I and Type II control. The Type - I control involves controlling both *d*- and *q*- axis currents separately using their own control loops. The DC voltage is kept fixed through the d-axis control loop. This control requires PWM for proper operation. On the other hand, in the Type - II control method, the phase angle between the STATCOM output voltage and the grid voltage is controlled. This control is suitable for line frequency switching.

F. Type - I control

The type - I control technique is typically used with IGBTs or MOSFETs which are suitable devices for PWM switching and is used in the modular multi-level converter (MMC) or the cascaded H-bridge (CHB) converters in conjunction with other capacitor charge balancing algorithms. Fig. 5 shows the block diagram for type – I control used in STATCOMs, for three phase systems. This control is designed around a particular choice of rotating reference frame, specifically, a

rotating reference frame with its d-axis aligned with phase A line voltage V_d , which makes $V_q = 0$. This linearizes equations (4) and (5) as:

$$P = \frac{3}{2}(V_d I_d) \tag{6}$$

$$Q = \frac{3}{2}(V_d I_q) \tag{7}$$

From equations (6) and (7), it is apparent that real power output is directly proportional to I_d, while the reactive power output is directly proportional to I_q. In general, the magnitude of the ac side terminal voltage remains fairly constant and V_d equals the peak magnitude of the voltage sine wave in the chosen reference frame. The command ${I_d}^*$ is obtained by comparing the actual dc bus voltage with the reference dc bus voltage. On the other hand the command ${I_q}^*$ is driven by the control objectives for the STATCOM, namely the provision of reactive power support, the regulation of the ac terminal voltage and unity power factor operation, that is ${I_q}^* = 0$.When the STATCOM provides reactive power support, the q-axis current reference is calculated as $I_q^* = \frac{2Q^*}{3V_d}$, where Q^* is the reactive power reference.

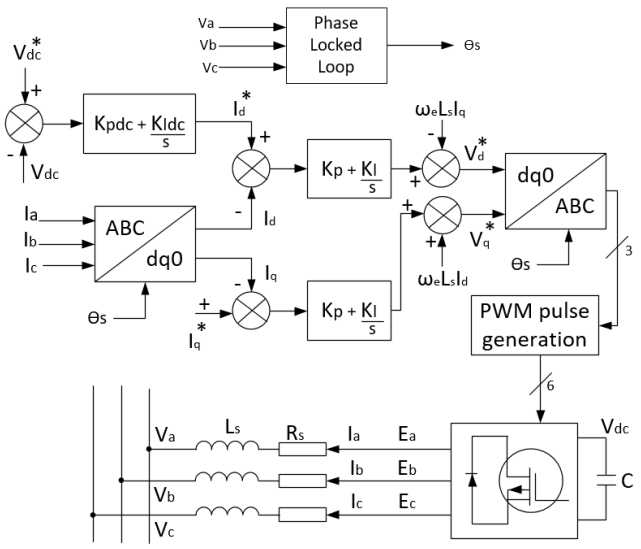

Fig. 5. STATCOM type - I control block diagram for a three phase system

When the STATCOM operates as a voltage regulator, it exploits the coupling between reactive power and line voltage, which is common in modern power systems. A PI controller can be used to obtain ${I_q}^*$ as

$$I_q^* = \left(K_{PV} + \frac{K_{IV}}{s}\right)(V_d^* - V_d) \tag{8}$$

The current references thus generated are given to current controllers along the respective axes to generate the voltage references for the converter. These are then transformed to the abc frame and compared with a high frequency triangle carrier wave to generate the PWM pulses for the power electronic switches.

G. Proportional Resonant (PR) Controllers

PI controllers have been widely utilized in VSCs for sinusoidal current injection to the grid. However, it is known that PI controllers have drawbacks, for example, steady-state tracking errors of sinusoidal command signals in the stationary frame, and distorted line currents due to presence of harmonics [11]. In literature, many techniques have been proposed to improve the performance of PI controllers, including an additional feedforward path for grid voltage[12], and multiple-state feedback[13]. These improvements do expand the bandwidth of the PI controller, however they make them operate closer to their stability limits. The proportional resonant (PR) controller, on the other hand, has started to replace the conventional PI controller in many applications, including grid-connected current control. The PR controller presents several advantages compared to the PI controller. These include lower total harmonic distortion (THD) in the current spectrum, and a simpler implementation, since it uses only the positive sequence component of the grid current [14]. The PR controller typically eliminates the steady state error by introducing an infinite gain at a selected resonant frequency. The controller consists of the proportional and the resonant parts, expressed by equation (9), whereby ω is a resonant frequency; K_i is the time constant integral, and K_p is the proportional gain which determines the gain margin and the phase of the bandwidth[15].

$$G_{PR}(s) = K_P + K_i\left(\frac{s}{s^2 + \omega^2}\right) \tag{9}$$

The performance of PI versus PR controllers has been compared in [16] while the design procedure for PR controllers have been addressed in [17]–[20].

H. PR Controller blocks

Fig. 6 shows the block diagram of the STATCOM controller for a single phase system. The output of a phase locked loop (PLL) block gives one active component and one reactive component. The active component is aligned in phase with the grid voltage, while the reactive component is in quadrature with the grid voltage. The error between the actual dc bus voltage (V_{dc}) and the reference (V_{dc}^*) is first calculated. This error is then fed to a PI controller, and its output is multiplied by the active component generated by the PLL block. Similarly, the estimated reactive component in the load current is multiplied by the reactive component generated by the PLL block. Both outputs of the multiplier blocks are added to give the current reference I_{ref}. This current is then compared with the actual inverter current, and the error is fed to a PR controller. Its output is then added to the grid voltage which gives the final reference voltage V_{ref}. This signal is used by the pulse width modulator for generating the switching signals of the VSC.

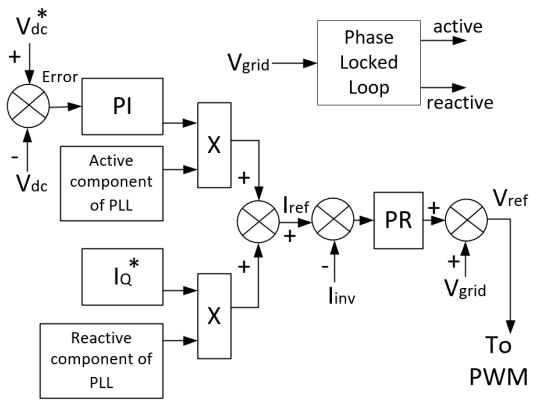

Fig. 6. STATCOM control for a single phase system

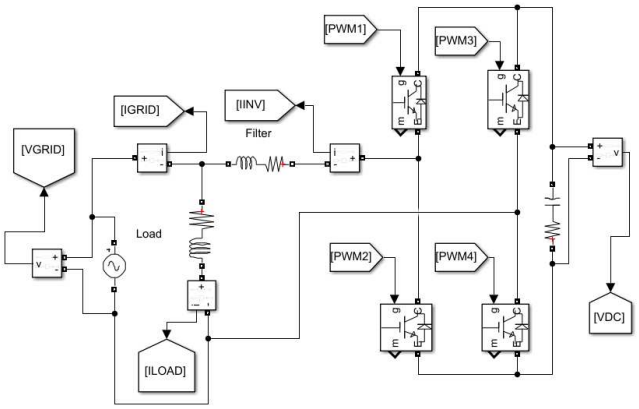

Fig. 7. SIMULINK model of a single phase STATCOM with an RC load

III. Tests and Results

The following simulations were carried out with Matlab /Simulink:

(1) Single phase STATCOM for reactive power control, using a PR controller

(2) Three phase STATCOM for reactive power control, using PI controller

A. Modeling and Simulation of a single phase STATCOM for reactive power control

Fig. 7 shows the Simulink model of a single phase STATCOM for reactive power compensation. The STATCOM, connected in shunt with the load provides reactive power to an RL load, or absorbs reactive power from an RC load. Thus, net reactive power transfer from the grid to the load is almost zero. The grid provides only active power, thus keeping the power factor to almost unity.

The STATCOM specifications are shown in TABLE II.

Rated Current = 2kVA/230 = 8.691 A

Reference DC voltage = 400V

Considering maximum drop across inductor = 5% of 230 = 11.5V

IX_l=11.5 V

Hence the calculated value of L = 4.2mH

TABLE II. STATCOM Specifications

Rated power	2 kVA
Output voltage	230 V
Frequency	50 Hz
dc bus capacitor	3000 μF
dc bus resistor	100 μΩ
PI controller gains	K_p= 0.5, K_i = 100
PR controller gains	K_p= 10, K_i = 400, ω=247
PWM carrier signal frequency	10 kHz

B. Simulation Results

TABLE III displays the results of simulations carried out using different loads. When the load is fully active, the reactive power taken by the load is zero. In the presence of the STATCOM, all the active power absorbed by the load is provided by grid, while all the reactive power is provided by the inverter. This holds true for RL, RC as well as RLC loads.

Fig. 8 shows the variation of V_GRID, I_GRID, I_LOAD, and I_INV with time with an RL load. It can be observed that the V_GRID and I_GRID are in phase, and thus the grid provides only active power. Similar graphs are obtained for RC and RLC loads.

TABLE III. Measured Active and Reactive power

Installed load	**Measured Active and Reactive power**					
	Grid		**Inverter**		**Load**	
Load	**P/W**	**Q/VAR**	**P/W**	**Q/VAR**	**P/W**	**Q/VAR**
R = 25 Ω	2158	-0.24	-45.4	0.238	2112	2.2e-12
R = 25 Ω L = 5mH	1906	0.13	-41.9	1757	1864	1758
R = 30 Ω L = 5mH	1132	2.18	-43.3	853.2	1089	855.2
R=12 Ω C=265μF	2248	-409.9	-48.9	-1791	2199	-2201
R = 25 Ω C=400μF	1965	-2.41	-46.9	-608.1	1918	-610.5

R = 25 Ω L=45mH C=400μF	3308	16.8	-49.1	-1631	3259	-1614
R = 50Ω L=75mH C=600μF	978	-3.2	-46.3	343.9	932	340

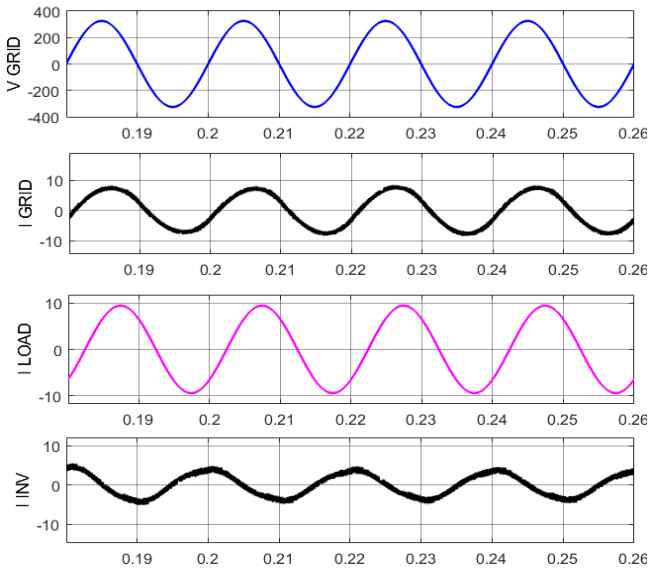

Fig. 8. Variation of V_GRID, I_GRID, I_LOAD, and I_INV with time with an RL load

C. Modeling and Simulation of a three phase STATCOM for reactive power control

The Simulink block diagram for a three phase STATCOM is shown in Fig. 9 . Different types of loads are simulated, for example fully resistive (R) as well as resistive and reactive (RL, RC and RLC), as shown in TABLE IV. It can be observed that, in all cases the active power consumed by the load is supplied by the grid (200 kW in this case), while the reactive power consumed/supplied by the load is supplied/absorbed by the inverter. Further simulations were carried out with different values of installed active load. Similar results were obtained. Vdc also settles to its reference value, after an initial transient of around 0.05 seconds. These results confirm the proper behaviour of the designed STATCOM, that is the provision/absorption of reactive power, while the grid provides only active power, thus keeping the power factor very close to unity. Fig. 10 shows the variation of V_GRID, I_GRID, I_LOAD, I_INV and Vdc with time with an RL three phase load. It is observed that after a short transient period of 0.1 second, the inverter current stabilizes. Similar graphs are obtained with RC and RLC loads.

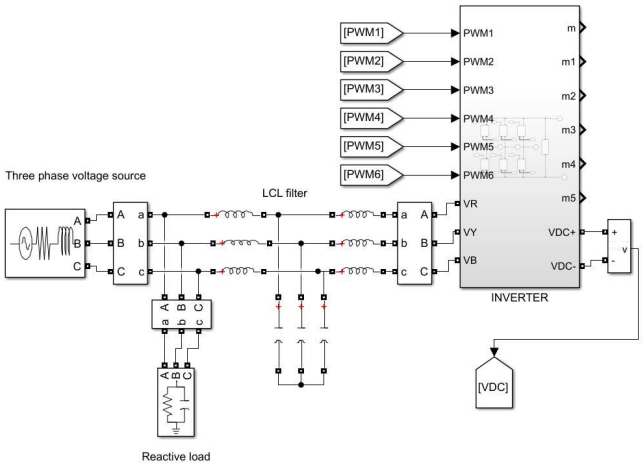

Fig. 9. Simulink model of a three phase STATCOM for reactive power control

TABLE IV. MEASURED ACTIVE AND REACTIVE POWER

Installed Reactive Load/VAR with Active Load of 200kW	**Measured Active and Reactive power**					
	Grid		**Inverter**		**Load**	
	P/W	**Q/VAR**	**P/W**	**Q/VAR**	**P/W**	**Q/VAR**
Nil	200k	-5285	-1911	-2612	200k	0
Inductive 100k	200k	-5725	-727.8	95k	200k	100k
Capacitive 75k	200k	-5489	-2274	-76k	200k	-75k
100k Inductive and 75k Capacitive	200k	-5296	-1633	22k	200k	25k

CONCLUSION

The reactive power transfer between the STATCOM and different loads (R, RL, RC, and RLC) was investigated for single phase and three phase power systems. Both PI and PR controllers were employed for the control of the STATCOM. The advantages of a PR controller, compared to a PI controller was briefly discussed. Simulations in Matlab/Simulink showed that for all combinations of loads, the STATCOM either provided reactive power to the load, or absorbed reactive power from the load. Thus, net reactive power transferred from the grid to the load was almost zero. The grid provided only active power, thus keeping the power factor close to unity. As further works, a photovoltaic (PV) or a wind grid connected system or even a hybrid of PV and wind grid connected system, incorporating a STATCOM, can be investigated for voltage regulation.

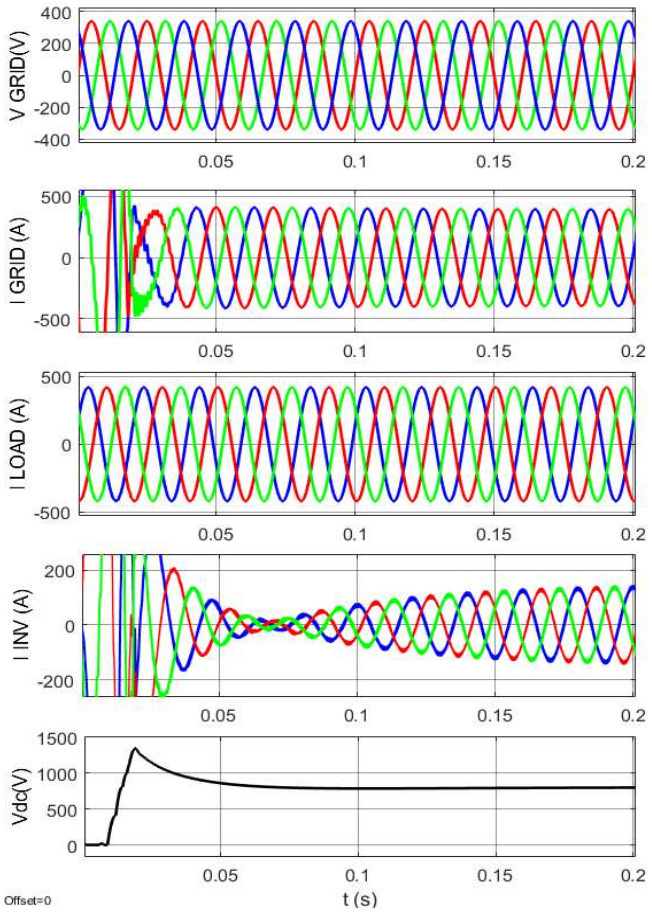

Fig. 10. Variation of V GRID, I GRID, I LOAD, I INV and Vdc with time for an RC three phase load

REFERENCES

[1] N. Hingorani and L. Gyugyi, *Understanding FACTS: Concepts and Technology of Flexible AC Transmission Systems*. Wiley-IEEE Press, 1999.

[2] B.-S. Chen and Y.-Y. Hsu, "An Analytical Approach to Harmonic Analysis and Controller Design of a STATCOM," *IEEE Transactions on Power Delivery*, vol. 22, no. 1, pp. 423–432, 2007, doi: 10.1109/TPWRD.2006.883016.

[3] A. R. M. Tenório, "SVCs vs STATCOMs," Paris, 2014.

[4] N. Mithulananthan, C. A. Canizares, J. Reeve, and G. J. Rogers, "Comparison of PSS, SVC, and STATCOM controllers for damping power system oscillations," *IEEE Transactions on Power Systems*, vol. 18, no. 2, 2003, doi: 10.1109/TPWRS.2003.811181.

[5] D. Ramirez, S. Martinez, F. Blazquez, and C. Carrero, "Use of STATCOM in wind farms with fixed-speed generators for grid code compliance," *Renew Energy*, vol. 37, no. 1, pp. 202–212, 2012, doi: https://doi.org/10.1016/j.renene.2011.06.018.

[6] U. Karaagac, I. Kocar, J. Mahseredjian, L. Cai, and Z. Javid, "STATCOM integration into a DFIG-based wind park for reactive power compensation and its impact on wind park high voltage ride-through capability," *Electric Power Systems Research*, vol. 199, p. 107368, 2021, doi: https://doi.org/10.1016/j.epsr.2021.107368.

[7] M. Rastogi, A. Ahmad, and A. H. Bhat, "Performance investigation of two-level reduced-switch D-STATCOM in grid-tied solar-PV array with stepped P&O MPPT algorithm and modified SRF strategy," *Journal of King Saud University - Engineering Sciences*, 2021, doi: https://doi.org/10.1016/j.jksues.2021.06.008.

[8] A. Benslimane, J. Bouchnaif, M. Essoufi, B. Hajji, and L. el Idrissi, "Comparative study of semiconductor power losses between CSI-based STATCOM and VSI-based STATCOM, both used for unbalance compensation," *Protection and Control of Modern Power Systems*, vol. 5, no. 1, 2020, doi: 10.1186/s41601-019-0150-4.

[9] B. Y. Vakadani and Y. Ponnam, "Grid power quality improvement in wind energy system using three and four leg inverter control," *Int J Eng Adv Technol*, vol. 8, no. 6 Special Issue 3, 2019, doi: 10.35940/ijeat.F1348.0986S319.

[10] C. Schauder and H. Mehta, "Vector analysis and control of advanced static VAR compensators," *IEE Proceedings C (Generation, Transmission and Distribution)*, vol. 140, no. 4, pp. 299–306, 1993.

[11] R. Teodorescu, F. Blaabjerg, M. Liserre, and A. Dell'Aquila, "A stable three-phase LCL-filter based active rectifier without damping," *Conference Record - IAS Annual Meeting (IEEE Industry Applications Society)*, vol. 3, pp. 1552–1557, 2003, doi: 10.1109/IAS.2003.1257762.

[12] M. Xue, Y. Zhang, Y. Kang, Y. Yi, S. Li, and F. Liu, "Full feedforward of grid voltage for discrete state feedback controlled grid-connected inverter with LCL filter," *IEEE Trans Power Electron*, vol. 27, no. 10, pp. 4234–4247, 2012, doi: 10.1109/TPEL.2012.2190524.

[13] G. M. Pelz, S. A. O. da Silva, and L. P. Sampaio, "Comparative analysis involving PI and state-feedback multi-resonant controllers applied to the grid voltage disturbances rejection of a unified power quality conditioner," *International Journal of Electrical Power & Energy Systems*, vol. 115, p. 105481, Feb. 2020, doi: 10.1016/J.IJEPES.2019.105481.

[14] M. Shahparasti, P. Catalán, N. F. Roslan, J. Rocabert, R. S. Muñoz-Aguilar, and A. Luna, "Enhanced Control for Improving the Operation of Grid-Connected Power Converters under Faulty and Saturated Conditions," *Energies 2018, Vol. 11, Page 525*, vol. 11, no. 3, p. 525, Feb. 2018, doi: 10.3390/EN11030525.

[15] X. Yuan, W. Merk, H. Stemmler, and J. Allmeling, "Stationary-frame generalized integrators for current control of active power filters with zero steady-state error for current harmonics of concern under unbalanced and distorted operating conditions," in *IEEE Transactions on Industry Applications*, 2002, vol. 38, no. 2. doi: 10.1109/28.993175.

[16] A. Timbus, M. Liserre, R. Teodorescu, P. Rodriguez, and F. Blaabjerg, "Evaluation of current controllers for distributed power generation systems," *IEEE Trans Power Electron*, vol. 24, no. 3, pp. 654–664, 2009, doi: 10.1109/TPEL.2009.2012527.

[17] T. D. C. Busarello, J. A. Pomilio, and M. G. Simoes, "Design Procedure for a Digital Proportional-Resonant Current Controller in a Grid Connected Inverter," in *2018 IEEE 4th Southern Power Electronics Conference, SPEC 2018*, 2019. doi: 10.1109/SPEC.2018.8636052.

[18] N. Zhang, H. Tang, and C. Yao, "A systematic method for designing a PR controller and active damping of the LCL filter for single-phase grid-connected PV inverters," *Energies (Basel)*, vol. 7, no. 6, 2014, doi: 10.3390/en7063934.

[19] R. Teodorescu, F. Blaabjerg, M. Liserre, and P. C. Loh, "Proportional-resonant controllers and filters for grid-connected voltage-source converters," *IEE Proceedings: Electric Power Applications*, vol. 153, no. 5, 2006, doi: 10.1049/ip-epa:20060008.

[20] M. Castilla, J. Miret, J. Matas, L. G. de Vicuña, and J. M. Guerrero, "Control design guidelines for single-phase grid-connected photovoltaic inverters with damped resonant harmonic compensators," *IEEE Transactions on Industrial Electronics*, vol. 56, no. 11, 2009, doi: 10.1109/TIE.2009.2017820.